

Quantitative colours of opaque minerals

A. PECKETT

Department of Geological Sciences, University of Durham, Durham DH1 3LE

Abstract

Anisotropic opaque minerals viewed in reflected light microscopy show two sets of colours: the colours seen in plane polarized light which change as the section is rotated on the microscope stage, and the colours seen between crossed polars which change as the analyser is uncrossed. These latter colours are known variously as polarization colours or anisotropic rotation tints, but are here referred to as anisotropy colours. They are commonly a diagnostic aid to correct mineral identification. All these colours occur as a consequence of the dispersion of the relative permittivity (dielectric) tensor—the variation in the values of the tensor with wavelength of incident light and in low symmetry crystals, the variation in the directions of the principal axes of the tensor with wavelength.

In this paper, it is shown that the colour seen in plane polarized light and the anisotropy colours can be predicted for any orientation of section, at any stage angle, and for any degree of uncrossing of the analyser by calculations based on the dielectric tensor values, and these predicted colours compare favourably with the observed values. Three minerals are studied in this paper as examples: stannite, covellite, and bournonite.

KEYWORDS: reflected light microscopy, colours, opaque minerals, stannite, covellite, bournonite.

Introduction

THE skilled ore microscopist makes extensive use of colour in the identification of opaque minerals. Colours are seen in plane polarized light, between crossed polars and between slightly uncrossed ('partly crossed') polars. Crossed polars have the NS analyser and EW polarizer exactly orthogonal. The amount of light reaching the eye is for most opaque minerals rather low and so the ore microscopist commonly uncrosses the analyser by a small angle, commonly $1-2^\circ$, to increase the amount of light. It is well-known that this changes the colour of the light reaching the eye (Cameron, 1961; Galopin and Henry, 1972). This facility, the ability to uncross the analyser, is one essential feature of reflected light microscopes usually absent in transmitted light microscopes.

In this paper, it is shown that the colours of opaque minerals viewed in plane polarized light at various stage angles, and the colours seen between exactly crossed and slightly uncrossed polars can be predicted by calculations based on the dispersion of the dielectric tensor. These calculations are an extension of the techniques used in an earlier paper on the use of matrices and tensors in optical mineralogy (Peckett, 1987).

Theory

It was shown in an earlier paper (Peckett, 1987), that the permitted vibration directions and relative intensity of light reflected from the surface of an anisotropic section can be calculated from the relative permittivity (dielectric) tensor. The nature of the light can be described by a two-element Jones vector of complex numbers $[E_x, E_y]$ which holds the amplitude and phase lag of waves parallel to the crosswires. If the differential phase lag between the two waves is zero then the reflected wave is plane polarized. However, in most cases, the reflected wave is elliptically polarized. Under exactly crossed polars, the intensity of light passing through the analyser is the product of E_x and its complex conjugate, E_x^* . If the analyser is rotated anti-clockwise by an angle ψ then the Jones vector is modified by the matrix multiplication $E' = RE$ where the matrix R is

$$\begin{bmatrix} \cos \psi & \sin \psi \\ -\sin \psi & \cos \psi \end{bmatrix}$$

In other words, the Jones vector on axes (x, y) which are the directions of the crosswires is transformed orthogonally to an axial system (x', y') with

vector components $[E_{x'}, E_{y'}]$, where y' is parallel to the analyser. The intensity of light passing through the analyser is then the product of $E_{y'}$ and its complex conjugate, $E_{y'}^*$.

Data sources

The reflectance data for the minerals in this study are available in the IMA/COM Quantitative Data File (Henry, 1977). Hereafter, specific mineral data are referenced by the symbol QDF, the key number in the file, and the name of the microscopist who made the determination. Subsequent to the initial preparation of this paper, a second edition by Criddle and Stanley (1986) has been published, replacing the first issue. The reflectances in air and oil were converted to relative permittivity (dielectric) tensor values using the Koenigsberger equations. The refractive indices of the immersion oil were calculated at various wavelengths using the manufacturers' recommended dispersion values, which follow a Cauchy law rather than the straight line graph for Cargille immersion liquids given in Galopin and Henry (1972).

The mathematical methods to be used here strictly speaking require the use of the relative permittivity tensor described on its principal axes. For most minerals such data do not exist. Since this paper is describing a method, it is felt adequate to use the partially oriented data of the IMA/COM data base. Thus for stannite the data of the IMA/COM file is assumed to be for the o - and e -vibrations, even if the data are actually the o - and e' -vibrations. The error is trivial provided the e' -vibration is close to the true e -vibration. For orthorhombic bournonite used here the data are oriented on the principal axes. If the method described here were to be extended to monoclinic and triclinic minerals, then the orientations of the principal vibrations with respect to the crystallographic axes as well as their reflectance values would have to be determined at every wavelength—a formidable task!

Calculation of colours

Two types of spectral data are used in these calculations. The measured reflectance data from the IMA/COM data bases yield the colours predicted to be seen in plane polarized light. The calculated intensities through crossed or uncrossed polars yield the predicted anisotropy colours.

The data are calculated at each of 16 wavelengths in the range 400–700 nm and then are converted to chromaticity co-ordinates, and the related parameters of luminance, dominant wave-

length and excitation purity by the standard CIE (1931) scheme which has been described in many texts. Grum and Bartleson (1980) give the tabulation of the spectral tristimulus values for the 2° observer which is for a narrow field of view thought most appropriate to microscopy. Illuminant C (blue-filtered tungsten light closely matching daylight) is assumed in this study. A condensed description of the calculation of chromaticity co-ordinates is given by Craig and Vaughan (1981). The integrations should strictly speaking be made continuously over the range 360–830 nm but in practice there is only a slight error in summation at 20 nm intervals over the range 400–700 nm.

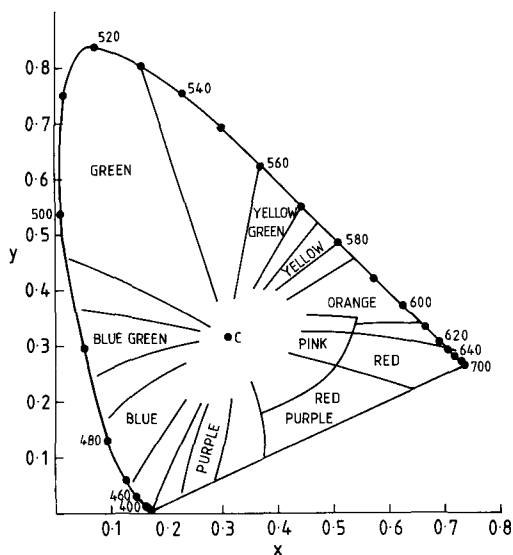


FIG. 1. CIE (1931) chromaticity diagram showing the colour names used in this paper. The areas are as defined by Kelly and Judd (1955) [in Grum and Bartleson, 1980], but may usefully be extended towards the Illuminant C. Unlabelled areas have colours described by the adjacent areas, e.g. bluish green for the area with $\lambda_d = 495$ nm.

It is believed that the chromaticity co-ordinates calculated here are accurate to ± 0.001 , luminances to $\pm 0.1\%$ and the dominant wavelength is accurate to 1 nm. A calculation from spectral data yields a set of chromaticity co-ordinates (x, y) . The name of the colour can be inferred from the CIE chromaticity diagram using the correlation of colour names and chromaticity co-ordinates (x, y) by Kelly and Judd (1955) as shown in texts such as Grum and Bartleson (1980) and reproduced here in a slightly modified form as Fig. 1.

Stannite

The reflectance of stannite increases slightly from the blue end of the visible spectrum to the red end and this is shown in Table 1. The data are from QDF 1.8140, Caye and Padeloup. The two principal vibrations of tetragonal stannite are both grey with olive-green tints (Ramdohr, 1980), greenish- or brownish-grey (Schouten, 1962) or olive-green (Galopin and Henry, 1972). The calculated dominant wavelengths are both close to 572 nm (yellow-brown) and the chromaticity co-ordinates of the *o*- and *e*-vibrations (actually *e'*) are plotted in Fig. 3.

The calculations here predict the colours of the stannite (100) section in the 45° position as shown in Fig. 2. Extracts of the numerical values at various steps in the calculations of this colour are given in Table 1. The reflectances of stannite at blue (400 nm) and red (700 nm) are listed for both *o*- and *e*-vibrations (using *e'* as synonymous for *e* for the purposes of this exercise) in air and under oil immersion. The refractive index of the immersion liquid is noted in Table 1 and the consequent values of the complex refractive index (*n-ik*) are shown as calculated from the Koenigsberger equations. The amplitude, *A*, and the phase lag, *φ*, of the reflected waves are calculated from the equation

$$\frac{1 - (n - ik)}{1 + (n - ik)} = A e^{i\phi}$$

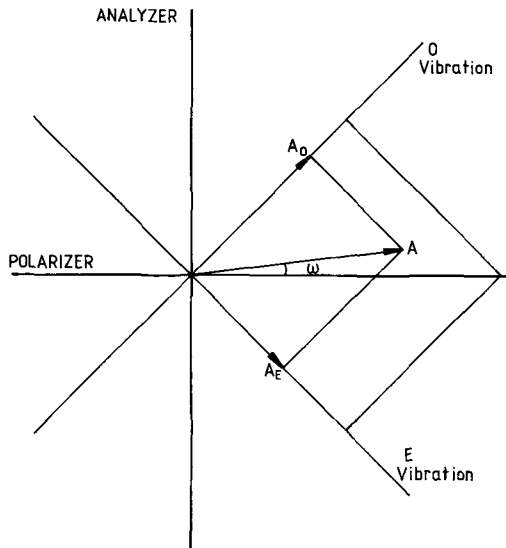


Fig. 2. Diagram to show how anisotropy colours are formed. The data are exaggerated for clarity. The data and key for stannite are given in Table 1.

for the cases where the principal vibrations are in their extinction position, i.e. parallel to the EW polarizer. The (100) section of stannite is considered to be in the 45° position as illustrated in Fig. 2, so that the amplitude of each permitted vibration is $1/\sqrt{2}$ of its value in the extinction positions.

Initially, we can ignore the differential phase lag between the two waves and consider the vector sum of the two vibrations to be a plane polarized wave in the orientation shown. Since the *o*-vibration has the higher reflectance, the angle *ω* shows the plane of the reflected wave to be oriented in NE quadrant. For blue light, the amplitudes *A_o* and *A_e* are 0.3376 and 0.3138 respectively and the vector sum has an amplitude of 0.4609 with *ω* = 2.1°. The reflectance is thus 22.12%. For red light, the amplitudes are 0.3715 and 0.3667, the vector sum is 0.5220, the reflectance is 27.3%, and the angle *ω* is 0.4°.

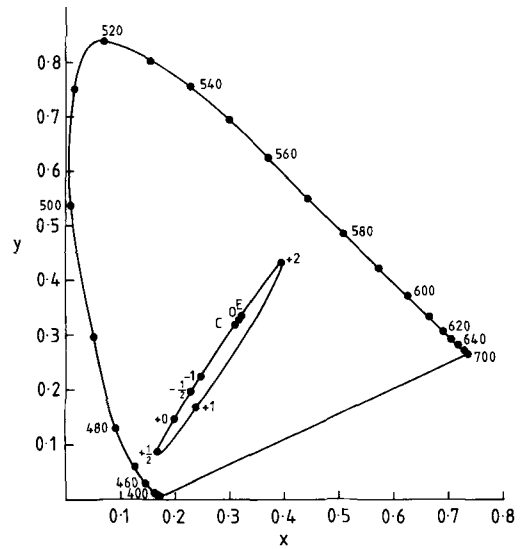


Fig. 3. CIE (1931) chromaticity diagram for a (100) section of stannite showing the colours in plane polarized light for the *e*- and *o*-vibrations (labelled E and O respectively), and the ellipse of anisotropy colours produced as the analyser is rotated. The numerical values of the rotation angle of the analyser are marked.

Allowance can be made for the fact that the reflected vibrations *A_o* and *A_e* are out of phase. As was shown in Peckett (1987), the Jones vector for the sum of the two vibrations yields the values in Table 1. The Stokes parameters calculated from the Jones vector show, as parameter *S₀*, the

Table 1. Calculation of the optical properties of stannite (100)

Blue light (400 nm)		Red light (700 nm)		Blue light (400 nm)		Red light (700 nm)	
o-vibration e-vibration o-vibration e-vibration				Jones vector for section in 45° position (Fig. 2) and analyser rotated through +j°			
R_{air}	22.8%	19.7%	27.6%	26.9%	$\frac{E_x}{A_x}, \frac{A_x}{x}$	0.4606	0.5220
R_{oil}	11.9%	8.9%	13.9%	13.2%	$\phi_{x'}$	rad. 2.630	2.825
n_{oil}	1.5384		1.5089		$\frac{E_y}{A_y}, \frac{A_y}{y}$	0.0195	0.0051
					$\phi_{y'}$	rad. 1.774	1.068
Complex refractive index ($\underline{n} - i\underline{k}$)				Intensity of light passing through analyser ($\frac{E_x}{x}, \frac{E_y}{y}, \frac{E_x^*}{x}, \frac{E_y^*}{y}$)			
\underline{n}	1.8827	1.9632	2.7296	2.7509		0.038%	0.003%
\underline{k}	1.2020	0.9994	1.0820	0.9917	Anisotropy colour		
Amplitude and phase lag of principal vibrations				$x = 0.172, y = 0.088, \underline{y} = 0.0015\%, \lambda_d = 463 \text{ nm}, \underline{p}_e = 81.1\%$			
A	0.4774	0.4439	0.5254	0.5187	Jones vector for section in 45° position (Fig. 2) and analyser rotated through +2°		
ϕ rad.	2.599	2.663	2.865	2.885	$\frac{E_x}{A_x}, \frac{A_x}{x}$	0.4608	0.5218
Jones vector for section in 45° position (Fig. 2)				$\phi_{x'}$ rad. 2.629			
$\frac{E_x}{A_x}, \frac{A_x}{x}$	0.4605		0.5220		$\frac{E_y}{A_y}, \frac{A_y}{y}$	0.0147	0.0155
$\phi_{x'}$ rad.	2.630		2.875		$\phi_{y'}$ rad.	1.106	0.156
$\frac{E_y}{A_y}, \frac{A_y}{y}$	0.0223		0.0062		Intensity of light passing through analyser ($\frac{E_x}{x}, \frac{E_y}{y}, \frac{E_x^*}{x}, \frac{E_y^*}{y}$)		
$\phi_{y'}$ rad.	1.911		1.875			0.022%	0.024%
Stokes parameters				Anisotropy colour			
S_0	0.2125		0.2725		$x = 0.400, y = 0.434, \underline{y} = 0.014\%, \lambda_d = 574 \text{ nm}, \underline{p}_e = 55.5\%$		
S_1	0.2115		0.2724		Jones vector for section in 45° position (Fig. 2) and analyser rotated through +15°		
S_2	0.0155		0.0035		$\frac{E_x}{A_x}, \frac{A_x}{x}$	0.4492	0.5051
S_3	-0.0135		-0.0054		$\phi_{x'}$ rad.	2.621	2.822
Angle ω				$\frac{E_y}{A_y}, \frac{A_y}{y}$			
	2.09°		0.37°		$\phi_{y'}$ rad.	0.1040	0.1317
Overall colour				Intensity of light passing through analyser ($\frac{E_x}{x}, \frac{E_y}{y}, \frac{E_x^*}{x}, \frac{E_y^*}{y}$)			
$x = 0.319, y = 0.329, \underline{y} = 26.4\%, \lambda_d = 572 \text{ nm}, \underline{p}_e = 5.8\%$							
Intensity of light passing through analyser ($\frac{E_x}{x}, \frac{E_y}{y}, \frac{E_x^*}{x}, \frac{E_y^*}{y}$)				Intensity of light passing through analyser ($\frac{E_x}{x}, \frac{E_y}{y}, \frac{E_x^*}{x}, \frac{E_y^*}{y}$)			
0.05%				0.004%			
Anisotropy colour				Anisotropy colour			
$x = 0.202, y = 0.147, \underline{y} = 0.005\%, \lambda_d = 466 \text{ nm}, \underline{p}_e = 61.1\%$				$x = 0.328, y = 0.343, \underline{y} = 1.61\%, \lambda_d = 572 \text{ nm}, \underline{p}_e = 12.2\%$			

intensity of the reflected wave. For blue light this is 21.25% and for red light it is 27.25%. The angle is now the angle between the major axis of the ellipse and the EW polarizer direction and this is 2.09° for blue light and 0.37° for red light. These calculations yield very similar results to the simplified case which disregarded ellipticity effects. Such is not the case in the later example of covelline where the differential phase lags may be quite large.

The calculations at all wavelengths yield a spectral reflectance $R(\lambda)$ ($= S_0(\lambda)$) from which the chromaticity co-ordinates can be calculated and

the resultant colour stated using Fig. 1. The resultant chromaticity co-ordinates lie on the line joining the colours of the two end-points for the o- and e-vibrations, as to be expected for a symmetric section.

The explanation for the origin of anisotropy or polarization colours is well known, e.g. Galopin and Henry (1972). It is illustrated here by the example of stannite with data in Tables 1 and 2. The analyser passes only that component of the reflected wave which is NS vibrating. Thus relative to the incident white light, the reflected light has a higher blue component than red and thus the

Table 2. Chromaticity co-ordinates (\bar{x}, \bar{y}), intensity (\bar{y} = luminance), dominant wavelength (λ_d), and excitation purity (P_e) of the anisotropy colours of a (100) section of stannite in the 45° position seen at various analyser settings (ψ).

ψ	\bar{x}	\bar{y}	\bar{y}	λ_d	P_e	colour
-45°	0.316	0.326	13.6%	572 nm	3.36%	pale brown = o-vibration
-10°	0.306	0.311	0.92%	471 nm	2.07%	pale blue
-2°	0.271	0.259	0.061%	468 nm	20.33%	blue
-1°	0.250	0.225	0.025%	467 nm	32.11%	blue
1°	0.231	0.195	0.013%	466 nm	42.63%	medium blue
0°	0.202	0.147	0.005%	465 nm	59.02%	medium blue
1°	0.172	0.088	0.0015%	462 nm	78.44%	deep blue
1°	0.242	0.170	0.0017%	432 nm	47.35%	violet
2°	0.400	0.434	0.014%	574 nm	43.45%	deep yellow-brown
10°	0.334	0.351	0.69%	572 nm	12.39%	brown
45°	0.321	0.333	12.89%	572 nm	5.90%	pale brown = e-vibration

anisotropy colour of stannite between exactly crossed polars is blue. Again using the simplified case by disregarding ellipticity effects, the intensity of blue light passing through an analyser is $R \sin^2 \omega$ which in this case is 0.03%, whereas for red light the value is 0.001%. The full calculation includes the effects of ellipticity and the intensity is given by (E_y, E_y^*) . This is 0.05% for blue light and 0.004% for red light. To calculate the anisotropy colour, the data are considered for all wavelengths in the visible range. Fig. 3 shows the chromaticity co-ordinates of the light passing through the perfectly crossed analyser and this is equivalent to a mixture of grey light and monochromatic blue light with a wavelength of 465 nm.

The effect of uncrossing the analyser can be seen qualitatively in Fig. 2 taken in conjunction with the data in Table 1. If the analyser is rotated anticlockwise by 0.4° then the red component of the reflected wave is completely extinguished and the reflected light appears lower in intensity but relatively more blue. As the analyser is rotated yet further, the section becomes very dark, but never completely extinguished, and when the analyser has been rotated to 2° , the small amount of light passing through the analyser is richer in red. Further rotation of the analyser causes more light, both red and blue components, to be transmitted, and the observed colour approaches that of the mineral seen in normal plane polarized light.

This rotation of the analyser is modelled mathematically by the rotation of the Jones vector using a matrix R as shown above in the theory section. The results of quantitative calculations of anisotropy colours are stated in Tables 1 and 2 for the (100) section in the 45° position and the chromaticity co-ordinates of the reflected light at various analyser settings are given graphically in

Fig. 3. The calculations predict that as the analyser is rotated clockwise (negative values of ψ), then the anisotropy colour becomes paler, but still predominantly blue until the section becomes almost colourless and then finally the normal olive-brown plane polarized light colour of the o-vibration. Very slight rotation of the analyser anticlockwise (positive values of ψ) produces a lowering of the intensity (from 0.005% when $\psi = 0^\circ$ to 0.002% when $\psi = \frac{1}{2}^\circ$), increasing saturation and a slight change in colour to a deeper blue (= violet) at about $\frac{1}{2}^\circ$ – 1° rotation ($\lambda_d = 437$ nm). Yet further rotation of the analyser to 2° produces a dull yellow-brown or khaki colour ($\lambda_d = 574$ nm) which then lightens and eventually the colour of the mineral as seen in plane polarized light for the e-vibration is reached when the angle ψ is 45° . The course of the change in colour is indicated by an ellipse in Fig. 3. The points labelled as angles of ψ are for this (100) section in the 45° position.

Ellipses similar in style to this were measured by Koritnig (1977) for 'oblique' sections of arsenopyrite and breithauptite. The IMA recommend the term 'anisotropic rotation tints' to describe these colours. In the author's opinion use of the term 'tint' (in contrast to the term 'shade') implies a colour not far from white. As is shown in Fig. 3, the excitation purity for the anisotropy colours can be very high and the term 'tint' seems inappropriate.

All other (hkl) sections of stannite have almost the same anisotropy colours although their intensities differ with the crystallographic orientation and the stage angle. A table in Galopin and Henry (1972) shows the anisotropy colours of a number of minerals under uncrossed polars and assigns each colour to a specific rotation angle of ψ . They are incorrect on this small point. The colour

sequences are correct, but the angles of ψ at which specific colours occur differ with the crystallographic orientation of the section.

These predicted anisotropy colours of stannite are similar to those observed by Galopin and Henry (1972) who state that the anisotropy colours under partially crossed polars are mauve-grey and yellowish to olive-brown. However, the predicted colours are only partly in accord with Ramdohr (1980) who states that the anisotropy colours are violet and slate green, and Schouten (1962) who also states colours of violet and green. The observation of a green colour is not predicted by these calculations since the ellipse in Fig. 3 always lies to the red side of the Illuminant C. The writer has never observed a green colour in stannite between crossed or uncrossed polars. It is possible that some of the examples of 'stannite' recorded in the literature are actually other members of the stannite group which include kesterite, stannoidite, etc.

Covellite

The two principal vibrations of hexagonal covellite are both blue, and their chromaticity co-ordinates are plotted in Fig. 4 with the points O and E for (x_o, y_o) and (x_e, y_e) respectively. The data

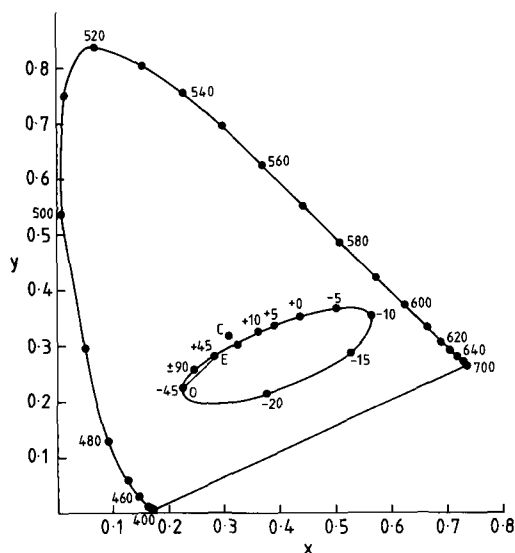


Fig. 4. CIE (1931) chromaticity diagram for a $(10\bar{1}0)$ section of covellite showing the colours in plane polarized light for the e' - and o -vibrations (labelled E and O respectively) and the ellipse of anisotropy colours produced as the analyser is rotated. The numerical values of the rotation angle of the analyser are marked.

are from QDF 1.1920.2, Piller. The dominant wavelengths are in the range 475–477 nm but the two waves differ markedly in both their excitation purity and luminance. For the darker blue ordinary wave this is $p_e = 0.364$, $Y_o = 6.9\%$ (where Y_o is the calculated luminance for the o -vibration) and for the lighter blue extraordinary wave it is $p_e = 0.118$, $Y_e = 23.5\%$.

Under crossed polars, covellite is a pale orange but according to Galopin and Henry (1972) it is pinkish-white, and according to Ramdohr (1980) it is orange to copper brown. The calculated chromaticity co-ordinates for this orange colour are plotted for a $(10\bar{1}0)$ section in the 45° position in Fig. 4. The dominant wavelength is 593 nm. On the colour names diagram Fig. 1 these co-ordinates are white but with an orange tint if the sectors are extended towards C along Munsell hue lines.

The reader with access to a polished mount of covellite is invited at this point to examine the section in the 45° position, rotate the analyser and list the changes in colour. The sequence of colours is from pale orange to deeper orange, reddish-orange, reddish-purple, purple, purple blue, and then the deep blue of the o -vibration. Rotation of the analyser in the opposite sense gives the colour sequence pale orange to near white and then pale blue which deepens to the blue of the e' -vibration. Such colour sequences were described by Green (1952). The chromaticity co-ordinates of these successive colours lie on or close to the ellipse drawn in Fig. 4. All sections of covellite, except the isotropic basal section, show the same colour sequence, but different crystallographically oriented sections will vary in their brightness.

The extreme anisotropy of covellite produces a broader and larger ellipse than the stannite example in Fig. 3. The figured examples of stannite and covellite which are typical of minerals with trigonal, hexagonal or tetragonal symmetry are for sections cut parallel to the unique axis and with the section in the $\alpha = 45^\circ$ position on the microscope stage. The chord joins the two points O and E, the colours of the o - and e' -vibrations seen in plane polarized light, and the end-points are at $\psi = \pm 45^\circ$. The co-ordinates of the anisotropy colour are on a tangent to the ellipse through the Illuminant C. For other orientations of sections, the two permitted vibrations are o and e' , with e' lying on the line O-E. The ellipse passes through the chromaticity co-ordinates of the o - and e' -vibrations and would by thus slightly different from the plotted examples. For other stage orientations, the end-points are at e with $\alpha = \psi$ and o with $\psi = -(90 - \alpha)$. As the orientation of a section closely approaches the basal section, the ellipse becomes smaller and narrower.

The chromaticity co-ordinates for the anisotropy colour for the $(10\bar{1}0)$ section of covellite (at $\psi = 0^\circ$) plot at (0.433, 0.355) with $\lambda_d = 593$ nm. The corresponding co-ordinates for a section near the isotropic (0001) lies at (0.381, 0.348) and its dominant wavelength is 589 nm. All other sections have the chromaticity co-ordinates of their anisotropy colours (at $\psi = 0^\circ$) lying along a curved line joining these two extreme points.

Bournonite

Bournonite is orthorhombic. In plane polarized light it appears white but with a detectable bireflectance and reflection pleochroism at grain and twin boundaries with undefined colours (Ramdohr, 1980). Schouten (1962) calls these pale bluish-green tints. The anisotropy colours are variegated according to these authors and readily picked out because of the parquet twinning. Uytendogaardt and Burke (1971) list 'pale blue, greenish grey, brownish yellow, dark brown and purplish' as anisotropy colours.

The chromaticity co-ordinates are plotted in Fig. 5 for the three principal vibration directions, labelled *a*, *b* and *c* to conform with the crystallographic axes. The data are from QDF 1.1060.1, Simpson. The data points lie on the blue side of the Illuminant C with dominant wavelengths in the range 480–482 nm. Symmetric sections of

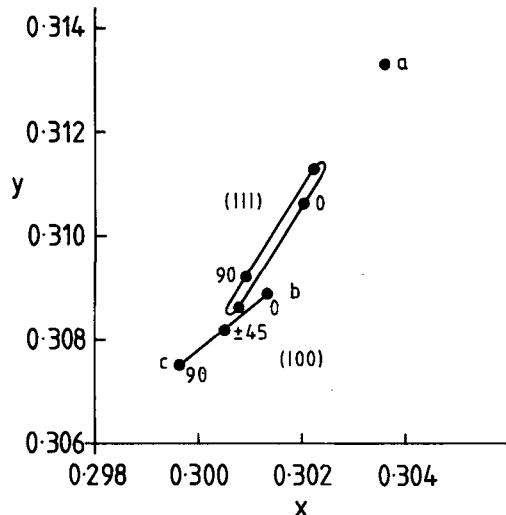


FIG. 5. Section of the CIE (1931) chromaticity diagram for bournonite showing the colours for sections (100) and (111) viewed in plane polarized light at various stage angles α . The symbols *a*, *b* and *c* are at the chromaticity co-ordinates of the three principal vibrations.

bournonite are those with indices of the forms $\{hk0\}$, $\{h0l\}$, $\{0kl\}$ and such sections have pleochroic schemes in plane polarized light such that the chromaticity co-ordinates of the reflected light at any stage angle α plot along a straight line joining end-points. All other $\{hkl\}$ sections are asymmetric sections (Galopin and Henry, 1972), and the chromaticity co-ordinates vary systematically around an ellipse. Since the vibration directions of asymmetric sections are dispersed (the vibration directions can vary with λ), a stage angle of α is referenced to the blue light vibration direction. Two examples are plotted in Fig. 5. Of necessity, since the pleochroism is not great, the diagram is an enlarged portion of the normal CIE chromaticity diagram.

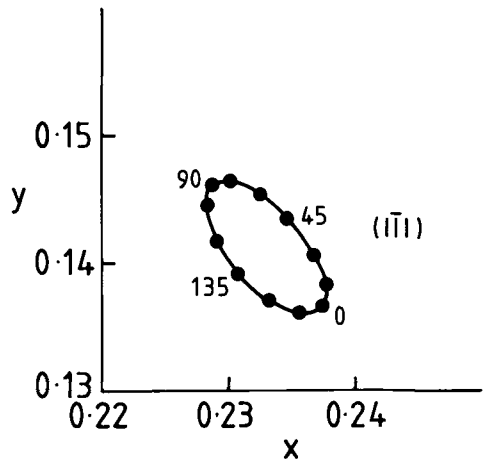


FIG. 6. Section of the CIE (1931) chromaticity diagram for bournonite showing the anisotropy colours of an asymmetric section $(1\bar{1}1)$ at various stage angles α .

For symmetric sections, the chromaticity co-ordinates of the anisotropy colours are constant with stage angle α with only a change in luminance, but for asymmetric sections the colours change as the stage is rotated. This is the origin of the occasional observation of different colours in adjacent quadrants as the stage is rotated. An example is plotted in Fig. 6 for a section of bournonite and the path of the change in chromaticity co-ordinates of the anisotropy colours is an ellipse. In general these ellipses are quite small and the colour changes are slight, but some orientations of sections especially those with low intensities can show greater colour changes in adjacent quadrants.

Fig. 7 shows the anisotropy colours of a randomly generated set of 100 oriented sections of bournonite, each section being viewed in the 45° position between exactly crossed polars. Many are deep blue and mid blue, some are purple blue, and some are green and yellow but with such low intensities that they would appear greenish-grey and brown. These calculated colours confirm the list of observed colours given by Uytendogaardt and Burke and listed above.

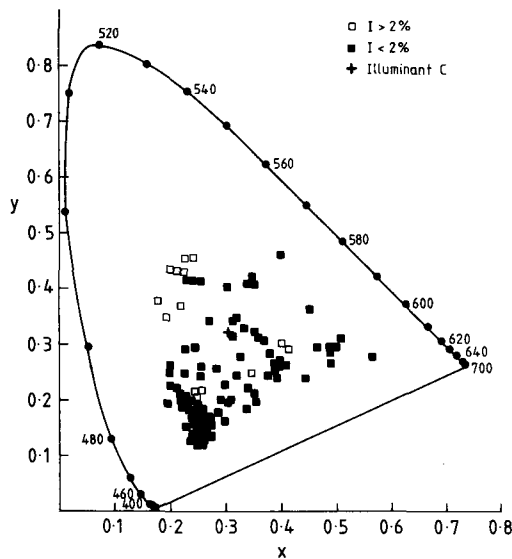


Fig. 7. CIE (1931) chromaticity diagram for bournonite showing the chromaticity co-ordinates of 100 random sections viewed in the 45° position between exactly crossed polars.

As with the earlier examples of covellite and stannite rotation of the analyser causes a brightening of the colours and a widening of the colour range.

Considering that bournonite is effectively white in plane polarized light, and orthorhombic in symmetry which precludes dispersion in the orientation of the tensor axes, the variegated anisotropy colours are quite remarkable.

Conclusions

The observed anisotropy colours of opaque minerals can be predicted by calculations based

on the dispersion of the dielectric tensor. A matrix method is used to compute the intensity of light which can pass through the analyser at each of 16 standard wavelengths in the visible range 400–700 nm and the chromaticity co-ordinates of the reflected spectrum can be calculated using the standard CIE (1931) scheme. The effect of uncrossing the analyser, which is a well-used procedure by ore microscopists can similarly be simulated by applying a rotation of the Jones vector prior to calculating the intensity. The predicted colours are closely similar to the observed values for most cases studied which include stannite, covellite, and bournonite.

Acknowledgements

The author wishes to acknowledge the encouragement he received from the late Roy Phillips MBE, during the past several years mutual study of the theory of episcopy. The author has benefited greatly from the comments of the reviewers of an earlier draft of this paper.

References

- Cameron, E. W. (1961) *Ore microscopy*. Wiley.
- Craig, J. R. and Vaughan, D. J. (1981) *Ore microscopy and ore petrography*. Wiley.
- Criddle, A. J. and Stanley, C. J. eds. (1986) *The quantitative data file for ore minerals*, 2nd ed. British Museum (Natural History).
- Galopin, R. and Henry, N. F. M. (1972) *Microscopic study of opaque minerals*. Published since 1975 by McCrone Research Assoc. Ltd. London.
- Green, L. H. (1952) *Econ. Geol.* **47**, 451–8.
- Grum, F. and Bartleson, C. J., eds. (1980) *Optical Radiation Measurements, 2, Color Measurement*. Academic Press.
- Henry, N. F. M., ed. (1977) *IMA/COM Quantitative Data File*. Applied Mineralogy Group, Mineralogical Society, London.
- Kelly, K. L. and Judd, D. B. (1955) *The ISCC-NBS Method of Designating Colors and a Dictionary of Color Names*. Nat. Bur. Standards Circular 553.
- Koritnig, S. (1977) *Neues Jahrb. Mineral. Mh.* 279–88.
- Peckett, A. (1987) *Mineral. Mag.* **51**, 655–63.
- Ramdohr, P. (1980) *The ore minerals and their intergrowths*, 2nd ed. Pergamon Press.
- Schouten, C. (1962) *Determinative tables for ore microscopy*. Elsevier.
- Uytendogaardt, W. and Burke, E. A. J. (1971) *Tables for microscopic identification of ore minerals*. Second revised edition. Elsevier.

[Manuscript received 1 December 1986;
revised 1 March 1988]